Theoretical modification on semiclassical distorted wave model and its application to the study of spin observables

K. Ogata and M. Kawai
Department of Physics, Kyushu University, Fukuoka 812-8581, Japan

Y. Watanabe* and Sun Weili
Department of Energy Conversion Engineering, Kyushu University, Kasuga, Fukuoka 816-8580, Japan

M. Kohno
Physics Division, Kyushu Dental College, Kitakyushu 803-8580, Japan
(Received 13 April 1999; published 1 October 1999)

The semiclassical distorted wave (SCDW) model of nucleon inelastic and charge exchange scattering at intermediate energies is modified to take accurate account of off-the-energy-shell matrix elements of the in-medium N-N interaction and explicit account of the exchange of colliding two nucleons, making use of the G matrix parametrized in coordinate representation. The effects of the modification on the double differential inclusive cross sections are discussed for the cases of $(p,p'x)$ and (p,nx) reactions on ^{90}Zr at 160 MeV. The modification enables the SCDW model to calculate spin observables. The depolarizations in ^{58}Ni$(p,p'x)$ at 80 MeV and ^{90}Zr$(p,p'x)$ and ^{90}Zr(p,nx) at 160 MeV by one- and two-step processes are calculated, and the result for ^{58}Ni$(p,p'x)$ is compared with experimental data. The calculated spin flips in $(p,p'x)$ and (p,nx) on ^{90}Zr are analyzed in terms of the effects of in-medium modification of the N-N interaction and the contributions of individual components of the effective interaction. [S0556-2813(99)03110-6]

PACS number(s): 24.10.Eq, 24.70.+s, 24.50.+g, 25.40.Ep

I. INTRODUCTION

Preequilibrium processes in nuclear reactions at intermediate energies are known to be dominated by multistep direct (MSD) processes. Quantum-mechanical models [1–3] and methods of simulation [4–7] have been proposed and applied to the analysis of preequilibrium MSD at intermediate energies with varying degrees of success. We have investigated MSD with a semiclassical distorted wave model, hereafter referred to as the SCDW model [8–11], based on the DWBA expansion of T-matrix elements as in the previous quantum-mechanical models. The cross section formula has no free adjustable parameter and allows a simple intuitive interpretation. We have applied the model to the calculation of double differential inclusive cross sections of $(p,p'x)$ and (p,nx) at intermediate energies taking account of up to three-step process. The results have been in overall good agreement with experimental data except at very forward angles and at large momentum transfers.

The SCDW model hitherto, however, has been based on the following two assumptions that need be examined. First, off-the-energy-shell matrix elements of N-N interaction are approximated by on-the-energy-shell ones whose squared moduli are replaced by a constant times free N-N scattering cross sections. Second, it is assumed that the effect of the exchange of colliding nucleons is included in the N-N scattering cross sections.

The first purpose of the present work is to remove the two assumptions to put the model on sounder theoretical foundations. We make use of the G matrix parametrized in coordinate representation by Dortmans and Amos [12,13], hereafter referred to as the DA G matrix, as the effective N-N interaction in the nuclear medium. The DA G matrix has an analytic form with parameters which are adjusted so that its on- and half-off-shell matrix elements reproduce those of the G matrix based on the Paris N-N potential [14].

The use of experimental free N-N cross sections has limited the application of the SCDW model so far to unpolarized cross sections. The modification described above enables one to calculate physical quantities beyond that limitation. The second purpose of this work is to calculate the spin observables for $(p,p'x)$ and (p,nx) reactions including one- and two-step processes. In particular, we analyze the depolarization D_{NN} and the spin flip S_{NN} in detail in terms of the number of steps of the process, the spin dependence of the effective interaction and the effects of its modification in the nuclear medium, hereafter referred to as in-medium effect.

In Sec. II, the formalism of the newly extended SCDW model is described and the formulas are given for unpolarized and polarized cross sections, and for some spin observables. The method and the input data of the numerical calculations are described in Sec. III. In Sec. IV the results of the numerical results are presented and discussed. A summary and conclusions are given in Sec. V.

II. FORMALISM

The starting point of the SCDW model is the DWBA series expansion of the T matrix for the reaction as already mentioned. The following three approximations are then

*Present address: Department of Advanced Energy Engineering Science, Kyushu University, Kasuga, Fukuoka 816-8580, Japan.

made [8–11]: the single particle model for the nucleus, the sum of the two-body interaction potentials for the residual interactions and the ''never-come-back'' assumption of MSD, viz. the number of excited target nucleons increases with the number of steps in MSD. Then the cross section for the reaction is given as an incoherent sum of the cross sections each of which corresponds to a number of steps in the process, since the final states of the system reached by different number of steps are different.

The T-matrix element of the one-step transition in which a target nucleon is excited from an initial single particle state $\phi_\alpha(\mathbf{r})$ to a final one $\phi_\beta(\mathbf{r})$ is given by

$$T_{\beta f,\alpha i}=\langle\chi_f(\mathbf{r}_0)\phi_\beta(\mathbf{r})|V_{12}(\mathbf{r}-\mathbf{r}_0)|\phi_\alpha(\mathbf{r})\chi_i(\mathbf{r}_0) - \phi_\alpha(\mathbf{r}_0)\chi_i(\mathbf{r})\rangle, \tag{2.1}$$

where the $\chi_{i,f}(\mathbf{r}_0)$ are the distorted waves for the leading particle (LP) at coordinate $\mathbf{r}_0$ in the initial and the final states, and $V_{12}(\mathbf{r}-\mathbf{r}_0)$ is the two-body interaction potential between LP and the struck target nucleon at $\mathbf{r}$. We assume for the moment that it is spin and isospin independent for simplicity. The cases of V_{12} including those variables will be discussed later. Equation (2.1) contains the exchange term explicitly. This is the first modification to the SCDW model. It should be noted that the use of V_{12} in the coordinate representation is an essential ingredient of the present model as will become clear in the formulation that follows.

With the T matrix of Eq. (2.1), the double differential inclusive cross section, hereafter referred to as the DDX, for one-step process of nucleon emission at energy $E_f\sim E_f+dE_f$ and into solid angle $d\Omega_f$ is given by

$$\frac{\partial^2\sigma^{1\,\mathrm{step}}}{\partial E_f\partial\Omega_f}=C\frac{k_f}{k_i}\sum_{\alpha,\beta}|T_{\beta f,\alpha i}|^2\delta(\epsilon_f-\epsilon_i), \tag{2.2}$$

where k_i and k_f are the asymptotic wave numbers of LP, ϵ_i and ϵ_f are the total energies of the system in the initial and the final states, respectively, and $C=4\mu^2/(2\pi\hbar^2)^2$. The delta function ensures the conservation of the total energies.

Putting $\mathbf{R}\equiv(\mathbf{r}+\mathbf{r}_0)/2$ and $\mathbf{s}\equiv\mathbf{r}-\mathbf{r}_0$, one can rewrite Eq. (2.2) as

$$\frac{\partial^2\sigma^{1\,\mathrm{step}}}{\partial E_f\partial\Omega_f}=C\frac{k_f}{k_i}\sum_{\alpha,\beta}|\langle\chi_f(\mathbf{R}-\mathbf{s}/2)\phi_\beta(\mathbf{R}+\mathbf{s}/2)|V_{12}(\mathbf{s})| \times\phi_\alpha(\mathbf{R}+\mathbf{s}/2)\chi_i(\mathbf{R}-\mathbf{s}/2)\rangle-\langle\chi_f(\mathbf{R}-\mathbf{s}/2) \times\phi_\beta(\mathbf{R}+\mathbf{s}/2)|V_{12}(\mathbf{s})|\phi_\alpha(\mathbf{R}-\mathbf{s}/2) \times\chi_i(\mathbf{R}+\mathbf{s}/2)\rangle|^2\times\delta(\epsilon_f-\epsilon_i). \tag{2.3}$$

We assume that the range b of V_{12} is short so that the integrand of Eq. (2.3) is only appreciable for small $|\mathbf{s}|<b$. We then make the following two approximations. One is the local density Fermi-gas (LFG) model for the nuclear states, and the other is the local semiclassical approximation (LSCA) for the distorted waves.

The LFG model for the nuclear states allows one to assume that the wave functions $\phi_\gamma(\gamma=\alpha,\beta)$ in Eq. (2.3) are plane waves within a small cell of size $|\mathbf{s}|<b$ so that

$$\phi_\gamma(\mathbf{R}\pm\mathbf{s}/2)\cong\phi_\gamma(\mathbf{R})e^{\pm i\mathbf{k}_\gamma\cdot\mathbf{s}/2}. \tag{2.4}$$

The LSCA for the distorted waves is essential to the SCDW model and is written as

$$\chi_c(\mathbf{R}\pm\mathbf{s}/2)\cong\chi_c(\mathbf{R})e^{\pm i\mathbf{k}_c(\mathbf{R})\cdot\mathbf{s}/2},\quad c=i,f, \tag{2.5}$$

for small $\mathbf{s}/2$, where $\mathbf{k}_c(\mathbf{R})$ is the local wave number given by [8]

$$\mathbf{k}_c(\mathbf{R})=\frac{\mu}{\hbar}\frac{\mathrm{flux}[\chi_c(\mathbf{R})]}{|\chi_c(\mathbf{R})|^2}. \tag{2.6}$$

With these two approximations, Eq. (2.3) becomes

$$\frac{\partial^2\sigma^{1\,\mathrm{step}}}{\partial E_f\partial\Omega_f}=C\frac{k_f}{k_i}\sum_{\alpha,\beta}|\langle\chi_f(\mathbf{R})\phi_\beta(\mathbf{R})|\phi_\alpha(\mathbf{R})\chi_i(\mathbf{R})\rangle \times\{\tilde{V}_{12}(\mathbf{q})-\tilde{V}(\mathbf{Q})\}|^2\delta(\epsilon_f-\epsilon_i), \tag{2.7}$$

where

$$\mathbf{q}\equiv\boldsymbol{\kappa}'-\boldsymbol{\kappa}\equiv[\mathbf{k}_\beta-\mathbf{k}_f(\mathbf{R})]/2-[\mathbf{k}_\alpha-\mathbf{k}_i(\mathbf{R})]/2, \tag{2.8a}$$

$$\mathbf{Q}\equiv\boldsymbol{\kappa}'+\boldsymbol{\kappa}\equiv[\mathbf{k}_\beta-\mathbf{k}_f(\mathbf{R})]/2+[\mathbf{k}_\alpha-\mathbf{k}_i(\mathbf{R})]/2, \tag{2.8b}$$

where $\boldsymbol{\kappa}$ ($\boldsymbol{\kappa}'$) is the relative momentum between the colliding nucleons in the initial (final) state, and $\mathbf{q}$ is the momentum transfer in the two-body center of mass system. $\tilde{V}_{12}$ is the Fourier transform of V_{12} defined by

$$\tilde{V}_{12}(\mathbf{k})=\int V_{12}(\mathbf{s})e^{-i\mathbf{k}\cdot\mathbf{s}}d\mathbf{s}. \tag{2.9}$$

Expanding the squared modulus in Eq. (2.7), one obtains

$$\frac{\partial^2\sigma^{1\,\mathrm{step}}}{\partial E_f\partial\Omega_f}=C\frac{k_f}{k_i}\int\int d\mathbf{R}d\mathbf{R}'\chi_f^*(\mathbf{R})\chi_i(\mathbf{R})\chi_f(\mathbf{R}') \times\chi_i^*(\mathbf{R}')\hat{K}(\mathbf{R},\mathbf{R}'), \tag{2.10}$$

where the kernel-hat $\hat{K}$ is defined by

$$\begin{aligned}\hat{K}(\mathbf{R},\mathbf{R}')&\equiv\sum_{\alpha,\beta}\phi_\beta^*(\mathbf{R})\phi_\beta(\mathbf{R}')\phi_\alpha(\mathbf{R})\phi_\alpha^*(\mathbf{R}') \times|\tilde{V}_{12}(\mathbf{q})-\tilde{V}_{12}(\mathbf{Q})|^2\delta(\epsilon_f-\epsilon_i)\\ &=\frac{1}{(2\pi)^6}\int_{k_\alpha<k_F(\mathbf{R})}d\mathbf{k}_\alpha e^{-i\mathbf{k}_\alpha\cdot(\mathbf{R}'-\mathbf{R})} \times\int_{k_\beta>k_F(\mathbf{R})}d\mathbf{k}_\beta e^{i\mathbf{k}_\beta\cdot(\mathbf{R}'-\mathbf{R})} \times|\tilde{V}_{12}(\mathbf{q})-\tilde{V}_{12}(\mathbf{Q})|^2\delta(\epsilon_f-\epsilon_i).\end{aligned} \tag{2.11}$$

It replaces the kernel K in the previous SCDW model defined by

$$K(\mathbf{R},\mathbf{R}') \equiv \frac{1}{(2\pi)^6} \int_{k_\alpha < k_F(\mathbf{R})} d\mathbf{k}_\alpha e^{-i\mathbf{k}_\alpha \cdot (\mathbf{R}'-\mathbf{R})} \times \int_{k_\beta > k_F(\mathbf{R})} d\mathbf{k}_\beta e^{i\mathbf{k}_\beta \cdot (\mathbf{R}'-\mathbf{R})} \delta(\epsilon_f - \epsilon_i), \tag{2.12}$$

which is a short range function of $\mathbf{R}-\mathbf{R}'$ [8–11]. The short range property of K is retained in $\hat{K}$ because of the short range nature of V_{12} which makes its Fourier transforms, $\tilde{V}_{12}(\mathbf{q})$ and $\tilde{V}_{12}(\mathbf{Q})$, slowly varying functions of the arguments, $\mathbf{q}$ and $\mathbf{Q}$.

The assumption of $\mathbf{R} \cong \mathbf{R}'$ allows one to use the LSCA to the $\chi_{i,f}(\mathbf{R}')$ in Eq. (2.10) and to obtain

$$\frac{\partial^2 \sigma^{1\,\mathrm{step}}}{\partial E_f \partial \Omega_f} = C \frac{k_f}{k_i} \frac{1}{(2\pi)^3} \int d\mathbf{R} |\chi_f(\mathbf{R})|^2 |\chi_i(\mathbf{R})|^2 \times \int \int_{k_\alpha < k_F(\mathbf{R}), k_\beta > k_F(\mathbf{R})} d\mathbf{k}_\alpha d\mathbf{k}_\beta |M^{\mathrm{new}}(\boldsymbol{\kappa}', \boldsymbol{\kappa})|^2 \times \delta[\mathbf{k}_\beta - \mathbf{k}_\alpha + \mathbf{k}_f(\mathbf{R}) - \mathbf{k}_i(\mathbf{R})] \delta(\epsilon_f - \epsilon_i), \tag{2.13}$$

where M^{new} is defined by

$$M^{\mathrm{new}}(\boldsymbol{\kappa}', \boldsymbol{\kappa}) \equiv \tilde{V}_{12}(\mathbf{q}) - \tilde{V}_{12}(\mathbf{Q}). \tag{2.14}$$

If one neglected the exchange term $\tilde{V}_{12}(\mathbf{Q})$, one would get

$$M'(\boldsymbol{\kappa}', \boldsymbol{\kappa}) \equiv \langle \boldsymbol{\kappa}' | V_{12}(\mathbf{s}) | \boldsymbol{\kappa} \rangle = \tilde{V}_{12}(\mathbf{q}), \tag{2.15}$$

which would have the form of the matrix element in the previous formulation of the SCDW model. This is only apparent, however, because in actual calculations in the previous SCDW model the squared modulus of the matrix element was replaced by the experimental N-N scattering cross section which did contain the effect of the exchange of colliding nucleons. In order to see this point more clearly, we rewrite M^{new} as

$$M^{\mathrm{new}}(\boldsymbol{\kappa}', \boldsymbol{\kappa}) = \int d\mathbf{s}\, e^{-i\boldsymbol{\kappa}' \cdot \mathbf{s}} V_{12}(\mathbf{s}) [e^{i\boldsymbol{\kappa} \cdot \mathbf{s}} - s^{-i\boldsymbol{\kappa} \cdot \mathbf{s}}] = \int d\mathbf{s}\, e^{-i\boldsymbol{\kappa}' \cdot \mathbf{s}} V_{12}(\mathbf{s}) [1 - P^x] e^{i\boldsymbol{\kappa} \cdot \mathbf{s}}, \tag{2.16}$$

where P^x is the exchange operator of the coordinates of the two nucleons, i.e.,

$$P^x \mathbf{s} = -\mathbf{s}. \tag{2.17}$$

In the previous formulation of the SCDW model [11], the matrix element was given by

$$M^{\mathrm{prev}}(\boldsymbol{\kappa}', \boldsymbol{\kappa}) \equiv \langle \boldsymbol{\kappa}' | v(\mathbf{s}) | \boldsymbol{\kappa} \rangle = \tilde{v}(\mathbf{q}), \tag{2.18}$$

where $v(\mathbf{s})$ is the ''two-body effective interaction.'' The squared modulus of the matrix element of $v(\mathbf{s})$ was then calculated in terms of the experimental two-nucleon scattering cross section. Comparing Eq. (2.16) with Eq. (2.18), one finds that this procedure is justified if

$$v(\mathbf{s}) = V_{12}(\mathbf{s})[1 - P^x], \tag{2.19}$$

since then $M^{\mathrm{prev}}(\boldsymbol{\kappa}', \boldsymbol{\kappa}) = M^{\mathrm{new}}(\boldsymbol{\kappa}', \boldsymbol{\kappa})$. One sees, therefore, that the ''two-body effective interaction'' in the previous formulation $v(\mathbf{s})$ contained the exchange operator, though only implicitly. Formally, however, it was treated as if it were a function only of $\mathbf{s}$. As a consequence, only the factorized kernel K appeared in the formulation. We see, however, that what is really needed is the kernel-hat $\hat{K}$. This is a defect of the previous formulation of the model, although its cross section formula is now justified as described above.

The second modification to the SCDW model is related to the energies of the colliding two nucleon system in the initial and the final states. It was shown in Ref. [11] that the argument of the energy delta function in Eq. (2.13) can be written as

$$\frac{\hbar^2}{2\mu}(k_\beta^2 - k_\alpha^2) + Q_{\alpha\beta} - \omega, \tag{2.20}$$

where ω is the energy transfer, $E_i - E_f$, $Q_{\alpha\beta} = S_\alpha - S_\beta$ is the reaction Q value and the S_γ ($\gamma = \alpha, \beta$) are the separation energies of the struck nucleon in the initial and the final nuclear states. It is obvious that the energy of the colliding N-N system is not conserved. As a consequence, the squared moduli of off-shell matrix elements of N-N interaction become necessary for the calculation of cross sections. In the SCDW model calculations hitherto, it was assumed that they were proportional to experimental N-N scattering cross sections. The validity of this assumption, however, needs be examined. It should also be noted that such a replacement restricts the application of the model to the calculations of unpolarized cross sections.

In this paper, we calculate the off-shell matrix elements explicitly. In the formulation described above, one needs an N-N effective interaction in coordinate representation for this purpose. We use the DA G matrix parametrized in coordinate representation by Dortmans and Amos [12,13].

The DA G matrix has the form

$$V_{12} = \sum_{ST} V_{12}^{ST} P^{ST}, \tag{2.21}$$

$$V_{12}^{ST} = V_C^{ST}(s) + V_{\mathrm{LS}}^{ST}(s) \boldsymbol{l} \cdot \mathbf{S} + V_{\mathrm{T}}^{ST}(s) S_{12}, \tag{2.22}$$

where S and T are the spin and the isospin, and $\boldsymbol{l}$ is the orbital angular momentum of relative motion of the two-body system. P^{ST} is the projection operator to ST channel and S_{12} is the usual tensor operator. The radial parts of the central and the spin-orbit components in Eq. (2.22) are sums of Yukawa forms, and that of the tensor component is a sum of s^2 times the Yukawa forms.

The ranges and the depths of individual components are given as energy and density dependent parameters, which are chosen so that the on- and half-off-shell matrix elements of the DA G matrix best fits those of the solution of the

Brückner-Bethe-Goldstone (BBG) equation for the Paris N-N potential [14]. The density dependence is given through the Fermi momentum k_F^G of the nuclear matter in which the BBG equation is solved.

With this G matrix, $M^{\rm new}(\boldsymbol{\kappa}',\boldsymbol{\kappa})$ is given by

$$M^{\rm new}(\boldsymbol{\kappa}',\boldsymbol{\kappa})=\sum_T \mathbf{A}(\nu_1'\nu_2'\nu_1\nu_2;T) \times\sum_S\sum_{MM'}(1/2m_1'1/2m_2'|SM') \times(1/2m_1 1/2m_2|SM)\times(\mathcal{M}_{\rm C}+\mathcal{M}_{\rm LS}+\mathcal{M}_{\rm T}), \tag{2.23}$$

where

$$A(\nu_1'\nu_2'\nu_1\nu_2;T)\equiv(1/2\nu_1'1/2\nu_2'|TT_3)(1/2\nu_1 1/2\nu_2|TT_3). \tag{2.24}$$

In Eqs. (2.23) and (2.24), the $m(m')$ are the z components of the spins, the $\nu(\nu')$ are the third components of the isopins of the LP 1 and the struck nucleon 2 in the initial (final) channel. M and M' are the the z components of the total spin S in the initial and the final state, respectively, and T_3 is the third component of the total isospin T of the two-nucleon system.

The matrix elements for the central, the spin-orbit, and the tensor components including both the direct and the exchange terms explicitly are given by

$$\mathcal{M}_{\rm C}=\{\tilde V_{\rm C}^{ST}(q)-(-)^{S+T}\tilde V_{\rm C}^{ST}(Q)\}\delta_{M,M'}, \tag{2.25}$$

$$\mathcal{M}_{\rm LS}=\frac{8\pi}{3}\kappa\sum_{a'}[(-)^{a'}(SM1a'|SM')\delta_{S,1} \times\{\tilde V_{\rm LS}^{ST}(q)[Y_1(\hat{\mathbf{q}}),Y_1(\hat{\boldsymbol{\kappa}})]_{1,-a'}+(-)^{S+T}\tilde V_{\rm LS}^{ST}(Q) \times[Y_1(\hat{\mathbf{Q}}),Y_1(\hat{\boldsymbol{\kappa}}')]_{1,-a'}\}], \tag{2.26}$$

$$\mathcal{M}_{\rm T}=-4\sqrt{2\pi}\sum_m[(-)^m(SM2-m|SM')\delta_{S,1} \times\{\tilde V_{\rm T}^{ST}(q)Y_{2m}(\hat{\mathbf{q}})-(-)^{S+T}\tilde V_{\rm T}^{ST}(Q)Y_{2m}(\hat{\mathbf{Q}})\}], \tag{2.27}$$

where Y are the spherical harmonics and $\tilde V_j^{ST}(k)$ (j=C, LS, and T) are given by

$$\tilde V_{\rm C}^{ST}(k)\equiv 4\pi\int s^2 ds\, j_0(ks)V_{\rm C}^{ST}(s)=4\pi\sum_i\frac{v_i^{\rm C}(R_i^{\rm C})^3}{1+(kR_i^{\rm C})^2}, \tag{2.28a}$$

$$\tilde V_{\rm LS}^{ST}(k)\equiv 4\pi\int s^3 ds\, j_1(ks)V_{\rm LS}^{ST}(s)=8\pi\sum_i\frac{v_i^{\rm LS}k(R_i^{\rm LS})^5}{\{1+(kR_i^{\rm LS})^2\}^2}, \tag{2.28b}$$

$$\tilde V_{\rm T}^{ST}(k)\equiv 4\pi\int s^2 ds\, j_2(ks)V_{\rm T}^{ST}(s)=32\pi\sum_i\frac{v_i^{\rm T}k^2(R_i^{\rm T})^7}{\{1+(kR_i^{\rm T})^2\}^3}, \tag{2.28c}$$

where R_i^j and v_i^j are, respectively, the range and the depth parameters of the ith component of the j=C, LS, and T potentials.

With this spin- and isospin-dependent DA G matrix, one gets the DDX for one-step process

$$\frac{\partial^2\sigma^{1\ \rm step}(\nu_1,\nu_1')}{\partial E_f\partial\Omega_f}=\frac{\mu^2}{2(2\pi\hbar^2)^2}\frac{k_f}{k_i}\frac{1}{(2\pi)^3}\int d\mathbf{R}|\chi_f(\mathbf{R})|^2|\chi_i(\mathbf{R})|^2\int\int_{k_\alpha<k_F(\mathbf{R}),k_\beta>k_F(\mathbf{R})}d\mathbf{k}_\alpha d\mathbf{k}_\beta \times\sum_{m_1,m_1'}\sum_{m_2,m_2'}\sum_{\nu_2}|M^{\rm new}(\boldsymbol{\kappa}',m_1'\nu_1'm_2'\nu_2'|\boldsymbol{\kappa},m_1\nu_1m_2\nu_2)|^2\delta[\mathbf{k}_\beta-\mathbf{k}_\alpha+\mathbf{k}_f(\mathbf{R})-\mathbf{k}_i(\mathbf{R})] \times\delta\left(\frac{\hbar^2}{2\mu}(k_\beta^2-k_\alpha^2)+Q_{\alpha\beta}-\omega\right), \tag{2.29}$$

which is merely the extension of Eq. (2.13) to the case in which V_{12} depends on the spin and the isospin.

Extension of the SCDW model to multistep processes has been made with the assumptions of the LFG model and the LSCA as for the one-step process and the additional assumption of the eikonal approximation to the intermediate Green functions [9]. The modification of the DDXs is quite similar to that for the one-step process described above. An explicit formula will be given later.

The modifications of the SCDW model described so far

not only put the model on sounder theoretical foundations, but also give the possibility of calculating various physical quantities other than the unpolarized DDX. In the following paper we calculate some spin observables in $(p,p'x)$ and (p,nx) reactions.

From Eq. (2.29) one can derive the DDX of a one-step process for specified spin directions of incoming and outgoing particles by lifting the summation over m_1' and the average over m_1

$$\frac{\partial^2\sigma^{1\ \mathrm{step}}(m_1,m_1',\nu_1,\nu_1')}{\partial E_f\partial\Omega_f}=\frac{\mu^2}{(2\pi\hbar^2)^2}\frac{k_f}{k_i}\frac{1}{(2\pi)^3}\int d\mathbf{R}|\chi_f(\mathbf{R})|^2|\chi_i(\mathbf{R})|^2\int\int_{k_\alpha<k_F(\mathbf{R}),k_\beta>k_F(\mathbf{R})}d\mathbf{k}_\alpha d\mathbf{k}_\beta$$
$$\times\sum_{m_2,m_2'}\sum_{\nu_2}|M^{\mathrm{new}}(\boldsymbol{\kappa}',m_1'\nu_1'm_2'\nu_2'|\boldsymbol{\kappa},m_1\nu_1m_2\nu_2)|^2\delta[\mathbf{k}_\beta-\mathbf{k}_\alpha+\mathbf{k}_f(\mathbf{R})-\mathbf{k}_i(\mathbf{R})]$$
$$\times\delta\left(\frac{\hbar^2}{2\mu}(k_\beta^2-k_\alpha^2)+Q_{\alpha\beta}-\omega\right). \tag{2.30}$$

Similarly, the modified expression for the partial cross section of a two-step process with specified spin directions of the incident and the outgoing particles is given by

$$\frac{\partial^2\sigma^{2\ \mathrm{step}}(m_1^{(1)},m_1'^{(2)},\nu_1^{(1)},\nu_1'^{(2)})}{\partial E_f\partial\Omega_f}=\frac{\mu^2}{(2\pi\hbar^2)^2}\frac{k_f}{k_i}\frac{1}{(2\pi)^6}\int dE_m\int d\mathbf{R}_1\int d\mathbf{R}_2|\chi_f(\mathbf{R}_2)|^2|\chi_i(\mathbf{R}_1)|^2$$
$$\times\int\int_{k_{\alpha_2}<k_F(\mathbf{R}_2),k_{\beta_2}>k_F(\mathbf{R}_2)}d\mathbf{k}_{\alpha_2}d\mathbf{k}_{\beta_2}\int\int_{k\alpha_1<k_F(\mathbf{R}_1),k_{\beta_1}>k_F(\mathbf{R}_1)}d\mathbf{k}_{\alpha_1}d\mathbf{k}_{\beta_1}$$
$$\times\frac{e^{-2\gamma_m|\mathbf{R}_2-\mathbf{R}_1|}}{|\mathbf{R}_2-\mathbf{R}_1|^2}\sum_{m_2^{(1)},m_2'^{(1)}}\sum_{m_2^{(2)},m_2'^{(2)}}\sum_{\nu_2^{(1)},\nu_2^{(2)}}\sum_{\nu_1'^{(1)}}|\mathcal{M}^{2\ \mathrm{step}}|^2$$
$$\times\delta[\mathbf{k}_{\beta_2}-\mathbf{k}_{\alpha_2}+\mathbf{k}_f(\mathbf{R}_2)-\mathbf{k}_m(\mathbf{R}_2)]\,\delta[\mathbf{k}_{\beta_1}-\mathbf{k}_{\alpha_1}+\mathbf{k}_m(\mathbf{R}_1)-\mathbf{k}_i(\mathbf{R}_1)]$$
$$\times\delta\left(\frac{\hbar^2}{2\mu}(k_{\beta_2}^2-k_{\alpha_2}^2)+Q_{\alpha_2\beta_2}-\omega_2\right)\delta\left(\frac{\hbar^2}{2\mu}(k_{\beta_1}^2-k_{\alpha_1}^2)+Q_{\alpha_1\beta_1}-\omega_1\right), \tag{2.31}$$

where

$$\mathcal{M}^{2\ \mathrm{step}}\equiv\sum_{m_1'^{(1)},m_1^{(2)}}M^{\mathrm{new}}(\boldsymbol{\kappa}'^{(2)},m_1'^{(2)}\,\nu_1'^{(2)}\,m_2'^{(2)}\,\nu_2'^{(2)}|\boldsymbol{\kappa}^{(2)}m_1^{(2)}\,\nu_1^{(2)}\,m_2^{(2)}\,\nu_2^{(2)})$$
$$\times M^{\mathrm{new}}(\boldsymbol{\kappa}'^{(1)}m_1'^{(1)}\,\nu_1'^{(1)}\,m_2'^{(1)}\,\nu_2'^{(1)}|\boldsymbol{\kappa}^{(1)}m_1^{(1)}\,\nu_1^{(1)}\,m_2^{(1)}\,\nu_2^{(1)}), \tag{2.32}$$

and the numbers 1 and 2 in the superscripts stand for the first and the second collision points, respectively. γ_m is the imaginary part of the local wave number of LP in the intermediate channel and $\omega_{1,2}$ are the energy transfers corresponding to the first and the second collisions, i.e., $\omega_1=E_i-E_m$, $\omega_2=E_m-E_f$, respectively. We neglect the spin and the isospin dependence of the distorting potential for LP in the intermediate state as we do for those in the initial and the final states. Then, the spin and the isospin of LP do not change in the intermediate state, i.e., $m_1^{(2)}=m_1'^{(1)}$ and $\nu_1^{(2)}=\nu_1'^{(1)}$. One sees from Eq. (2.32) that two paths with different $m_1'^{(1)}$ interfere.

With Eqs. (2.30) and (2.31), we can calculate four polarized cross sections, i.e., $\sigma_{\uparrow\uparrow}$, $\sigma_{\uparrow\downarrow}$, $\sigma_{\downarrow\uparrow}$, and $\sigma_{\downarrow\downarrow}$, where the left (right) arrow stands for the spin direction of the incident (emitted) particle. Once these four partial cross sections are calculated, the polarization P, the vector analyzing power A, the depolarization D_{NN}, and the spin flip S_{NN} can be obtained by the combination of them. We fix the axis of quantization for the spins by taking the right hand coordinate system with z axis perpendicular to the scattering plane, and the y axis in the direction of incident beam. Then, P, A, D_{NN}, and S_{NN} are given by

$$P\equiv\frac{\mathrm{Tr}(TT^\dagger\sigma_z)}{\mathrm{Tr}(TT^\dagger)}=\frac{\sigma_{\uparrow\uparrow}-\sigma_{\uparrow\downarrow}+\sigma_{\downarrow\uparrow}-\sigma_{\downarrow\downarrow}}{\sigma_{\uparrow\uparrow}+\sigma_{\uparrow\downarrow}+\sigma_{\downarrow\uparrow}+\sigma_{\downarrow\downarrow}}, \tag{2.33a}$$

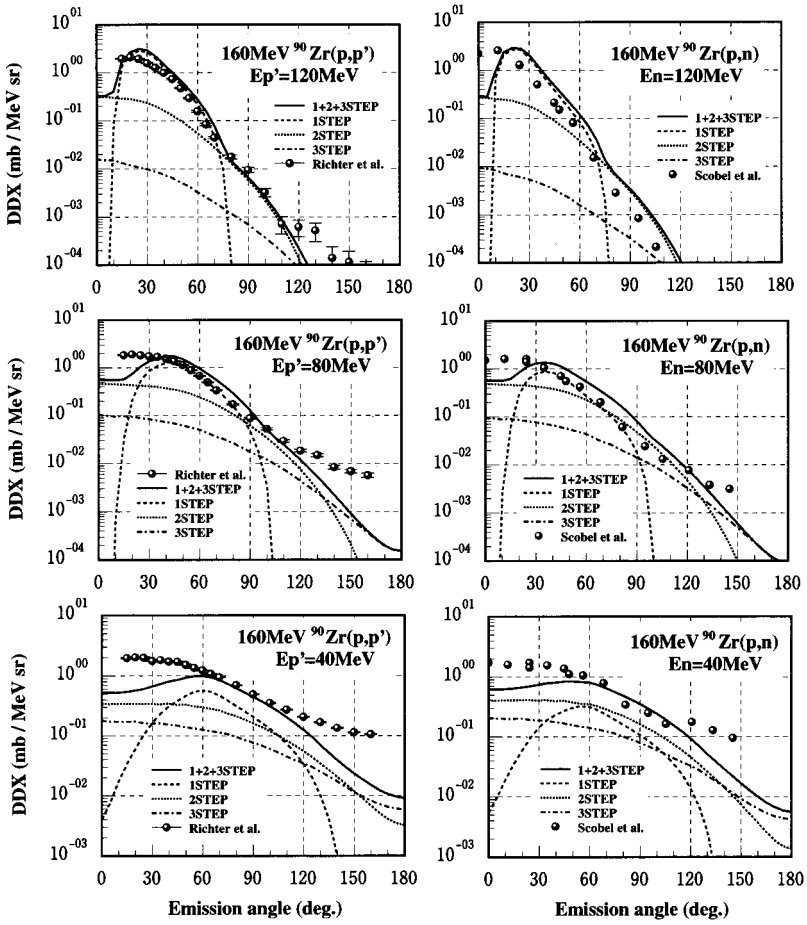

FIG. 1. Comparison between the calculated and experimental DDXs for $(p,p'x)$ and (p,nx) on ^{90}Zr at 160 MeV for three emission energies of 120, 80, and 40 MeV. The left (right) panel corresponds to $(p,p'x)$ $[(p,nx)]$. The cross sections of one-, two-, and three-step processes are represented by dashed, dotted, and dash-dotted lines, respectively. The solid curves are the sum of them. All of the calculations use the in-medium DA G matrix. The data are from Ref. [22] for $(p,p'x)$ and Ref. [23] for (p,nx).

$$A \equiv \frac{\mathrm{Tr}(T\sigma_z T^\dagger)}{\mathrm{Tr}(TT^\dagger)} = \frac{\sigma_{\uparrow\uparrow}+\sigma_{\uparrow\downarrow}-\sigma_{\downarrow\uparrow}-\sigma_{\downarrow\downarrow}}{\sigma_{\uparrow\uparrow}+\sigma_{\uparrow\downarrow}+\sigma_{\downarrow\uparrow}+\sigma_{\downarrow\downarrow}}, \quad (2.33b)$$

$$D_{NN} \equiv \frac{\mathrm{Tr}(T\sigma_z T^\dagger \sigma_z)}{\mathrm{Tr}(TT^\dagger)} = \frac{\sigma_{\uparrow\uparrow}-\sigma_{\uparrow\downarrow}-\sigma_{\downarrow\uparrow}+\sigma_{\downarrow\downarrow}}{\sigma_{\uparrow\uparrow}+\sigma_{\uparrow\downarrow}+\sigma_{\downarrow\uparrow}+\sigma_{\downarrow\downarrow}}, \quad (2.33c)$$

$$S_{NN} \equiv \frac{1}{2}(1-D_{NN}) = \frac{\sigma_{\uparrow\downarrow}+\sigma_{\downarrow\uparrow}}{\sigma_{\uparrow\uparrow}+\sigma_{\uparrow\downarrow}+\sigma_{\downarrow\uparrow}+\sigma_{\downarrow\downarrow}}, \quad (2.33d)$$

where σ_z is the z component of the Pauli spin matrix.

We emphasize that the axis of the spin quantization is fixed throughout multistep processes. This greatly simplifies the calculation. In contrast, calculations become very complicated with an effective interaction in momentum representation because the quantization axis for the spin depends on the direction of the propagation of LP in the intermediate state and the momentum of the struck target nucleon. Note that the latter dependence exists even in a one-step process. In practice, this is treated approximately, for example, with the so-called optimal momentum assumption.

III. NUMERICAL CALCULATION

We adopted the global optical potentials of Schwandt *et al.* [15] for $E_{\mathrm{LP}} \geqslant 80$ MeV and of Walter and Guss [16] for $E_{\mathrm{LP}} < 80$ MeV, where E_{LP} is the energy of the leading particle in the laboratory frame. For neutron, we slightly modified the potential of Ref. [15] in the way of Madland [17].

We assumed that those potentials are equivalent local potentials of the ''true'' nonlocal optical potentials, and multiplied the Perey factor [18] to each distorted wave to take account of the reduction of its amplitude due to the nonlocality of the potential. The range of nonlocality β was taken to be 0.85 fm. We did not include the spin-orbit terms of the optical potentials as already mentioned. The effects of this approximation on the calculated spin observables will be examined in the next section.

For nuclear density $\rho(\mathbf{R})$, we used Negele's parameter set of Woods-Saxon forms [19] and we assumed the proton and the neutron densities to be given by $Z/A\rho(\mathbf{R})$ and $N/A\rho(\mathbf{R})$, respectively. Then the corresponding local Fermi momenta, necessary for calculating unpolarized and polarized cross sections, were obtained by

$$\begin{cases} k_F^{(p)} = (3\pi^2 \rho(\mathbf{R}) Z/A)^{1/3}, \\ k_F^{(n)} = (3\pi^2 \rho(\mathbf{R}) N/A)^{1/3}, \end{cases} \quad (3.1)$$

which were also used as an input parameter for calculating the DA G matrix. To calculate the DDXs, we carried out the multifold integrals by means of Monte Carlo integration method with quasirandom numbers [20,21].

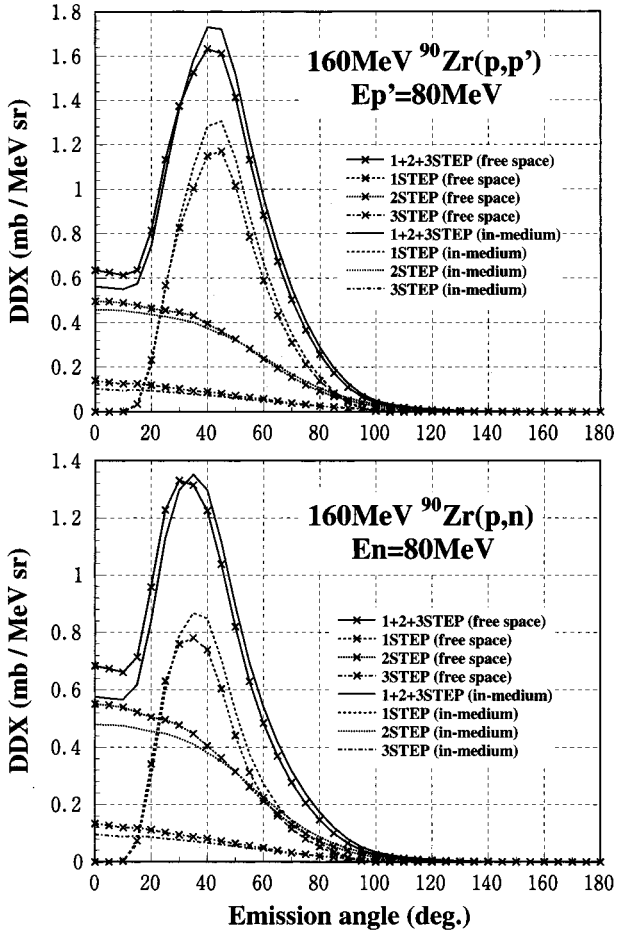

FIG. 2. The DDXs calculated with ''free space'' DA *G* matrix, i.e., with $k_F^G=0$ (lines with crosses) for $(p,p'x)$ and (p,nx) on ^{90}Zr at 160 MeV for the emission energy of 80 MeV, compared with those shown in Fig. 1 including the in-medium effect (lines without crosses). The upper (lower) panel corresponds to $(p,p'x)$ [(p,nx)]. The meaning of the lines is the same as in Fig. 1.

IV. RESULT AND DISCUSSION

A. Double differential cross section

Figure 1 shows the calculated DDXs of $(p,p'x)$ and (p,nx) on ^{90}Zr at 160 MeV compared with the experimental data [22,23]. The dashed, dotted, and dash-dotted lines represent cross sections of one-, two-, and three-step processes, respectively, and the solid lines are the sum of them. The calculated cross sections have just the same features as those of our previous work [11] and are in overall good agreement with data except at very small and large angles for both $(p,p'x)$ and (p,nx).

In order to clarify the in-medium effect on the DDX, we carried out the calculations with the DA *G* matrix putting $k_F^G=0$, hereafter referred to as the ''free space'' calculations. The typical results are shown in Fig. 2, with those of the in-medium calculation for comparison. Crosses on the lines stand for the ''free space'' calculation. Note that the DDXs are plotted in linear scale. One sees that the in-medium effects on the DDXs are only less than about 10%, in agreement with the conclusion of Ref. [11]. The reason for this is, as mentioned in Ref. [11], that the scattering takes place mainly in the nuclear surface region in which the local Fermi momentum is relatively small. We also calculated the DDXs using the *t* matrix parametrized by Love and Franey [24,25] for both on- and off-shell matrix elements and the results were quite close to those of ''free space'' calculation.

B. Spin observables

We first examined the effects of spin-orbit terms of optical potentials that we neglected in our calculation. For this purpose, we made test DWBA calculations of the contribution of the one-step process to the four spin observables given by Eq. (2.33) with the spin-orbit terms in the distorting potentials and a spin-independent *N-N* interaction, Yukawa potential of range 1 fm. The calculated spin observables are then only affected by the spin-orbit coupling in the distorting potentials. We used a method often adopted in DWBA calculations of $(p,p'x)$ and (p,nx) to the continuum [1,26]. The

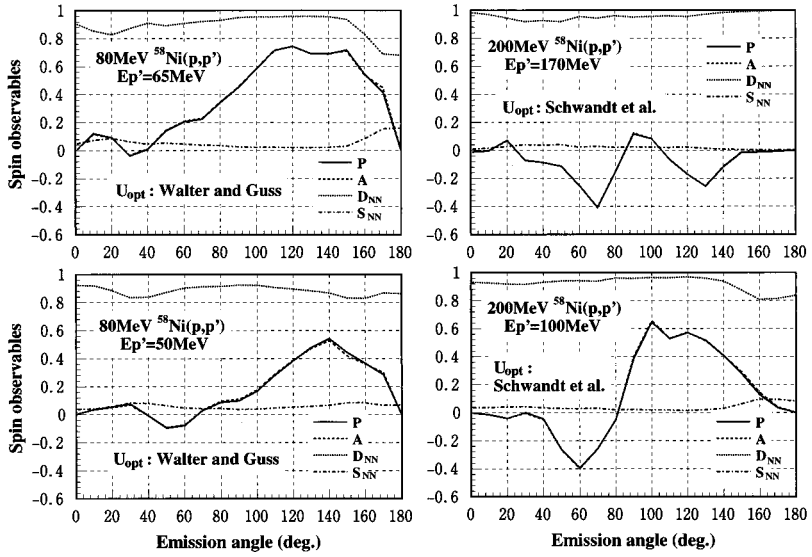

FIG. 3. Spin observables calculated with the use of DWBA code DW81 [27] with the spin-orbit terms of the distorting potentials and no spin dependence of *N-N* force for ^{58}Ni$(p,p'x)$ at $E_p=80$ MeV and $E_{p'}=65$ MeV and 50 MeV (left panel), and at $E_p=200$ MeV and $E_{p'}=170$ MeV and 100 MeV (right panel). The solid, dashed, dotted, and dash-dotted lines represent the polarization *P*, the vector analyzing power *A*, the depolarization D_{NN}, and the spin flip S_{NN}, respectively. Note that *A* and *P* are very close to each other.

cross section was calculated as the incoherent sum of the cross sections of the excitation of one-particle one-hole states. For each occupied bound single particle state α, those spherical Nilsson orbits that are at the given excitation energy from α were selected to find proper angular momenta and parities of the final single particle states. The radial part of the single particle wave function was calculated in a Woods-Saxon potential whose depth was adjusted so that for a bound state its separation energy is reproduced, and for a state in the continuum to make it is barely bound at 0.2 MeV. We carried out the calculations for the cases of $(p,p'x)$ on ^{58}Ni at 80 and 200 MeV, using the DWBA code DW81 [27].

The results are shown in Fig. 3. One sees that the polarization P and the vector analyzing power A have finite values. This indicates that our model cannot be used for the calculation of these quantities. In contrast, the depolarization D_{NN} and the spin flip S_{NN} deviate very little from 1 and 0, respectively. This implies that the neglect of the spin-orbit potentials in the distorting potentials is justified in the calculation of D_{NN} and S_{NN} in a one-step process.

The method described above is not applicable to quantitative tests for intermediate states in multistep processes. Qualitatively, however, the overall effect of this approximation is probably not so important because (a) the distance of propagation of LP in the potential in the intermediate state is short and (b) spin-orbit coupling potentials are localized in the surface of the nucleus, therefore do not much affect the intermediate propagation in the nuclear interior. In addition, the multistep cross sections are small compared to the one-step ones except at very small and large angles.

We show the calculated and experimental [28] D_{NN} for $(p,p'x)$ on ^{58}Ni at 80 MeV in Fig. 4, and the corresponding result and data [29] for the DDX in Fig. 5. In Fig. 4, the dashed and solid lines are the results of one-step and one-plus-two-step processes, respectively. Crosses on the lines indicate that in-medium effects are not included, i.e., using the ''free space'' DA G matrix. The interference terms between the different paths in two-step process discussed in Sec. II turned out to be negligibly small.

The calculated D_{NN} agrees with the experimental data in the sign and roughly the magnitude at forward angles. Also, the angular dependence that monotonically decreasing toward large angles is qualitatively reproduced. The agreement seems reasonable considering the simplicity of the model, although the calculation underpredicts D_{NN} at 60°, the maximum angle of the experimental data. The ''free space'' calculations give quite similar results as the calculations with in-medium effect, except still smaller D_{NN} at backward angles.

From Fig. 4, one sees that the contribution of two-step process is quite small in the middle angular region. This is because, as one can see from Fig. 5, the contribution of the two-step process to the cross section is much smaller than that of the one-step process there. At small angles where the two-step cross section is comparable to the one-step one, the two-step contribution is also appreciable to D_{NN}. At very forward angles, say 0°, the D_{NN} is quite different from that of one-step process. The reliability of the present calculation, however, is questionable there.

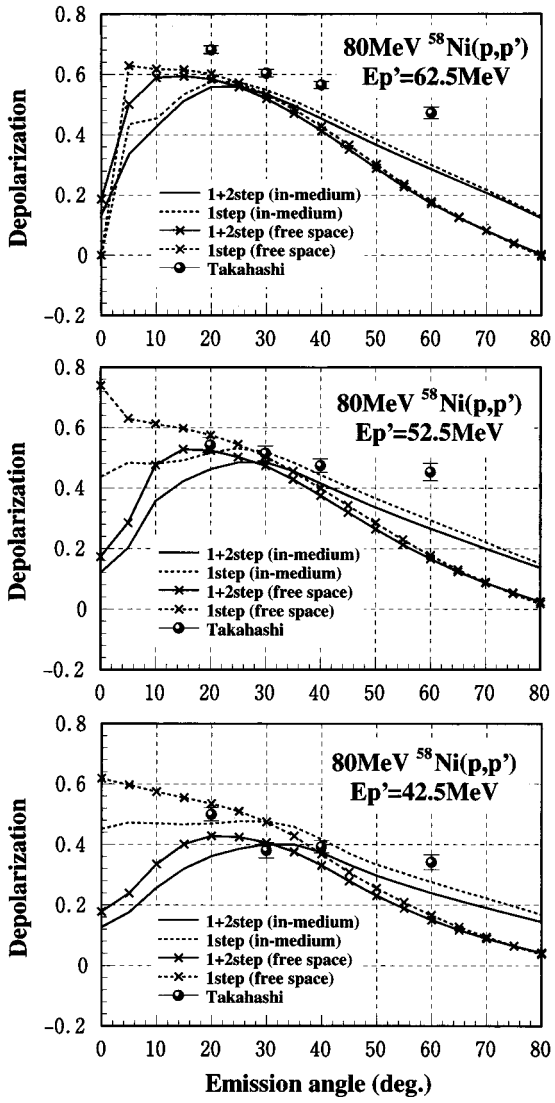

FIG. 4. Comparison between the theoretical and the measured D_{NN} for ^{58}Ni$(p,p'x)$ at $E_p = 80$ MeV and $E_{p'} = 62.5$, 52.5, and 42.5 MeV. The one-step and one-plus-two-step calculations with the DA G matrix are represented by the dashed and solid lines, respectively. The crosses on the lines stand for the ''free space'' calculation. The data are from Ref. [28].

Figure 6 shows calculated D_{NN} for $(p,p'x)$ and (p,nx) on ^{90}Zr at 160 MeV. For $(p,p'x)$, the calculated D_{NN} has quite similar features as in Fig. 4, while for (p,nx) it is very different from Fig. 4 in that the in-medium effect can now be clearly seen. In order to see this in more detail, we analyzed the calculated spin flip in terms of different components of the DA G matrix in the following representation:

$$V_{12} = V_0(s) + V_\sigma(s)\boldsymbol{\sigma}_1\cdot\boldsymbol{\sigma}_2 + V_\tau(s)\boldsymbol{\tau}_1\cdot\boldsymbol{\tau}_2 + V_{\sigma\tau}(s)\boldsymbol{\sigma}_1\cdot\boldsymbol{\sigma}_2\boldsymbol{\tau}_1\cdot\boldsymbol{\tau}_2 + V_{\mathrm{LS}}(s)\boldsymbol{l}\cdot\mathbf{S} + V_{\mathrm{LS}\tau}(s)\boldsymbol{l}\cdot\mathbf{S}\boldsymbol{\tau}_1\cdot\boldsymbol{\tau}_2 + V_{\mathrm{T}}(s)S_{12} + V_{\mathrm{T}\tau}(s)S_{12}\boldsymbol{\tau}_1\cdot\boldsymbol{\tau}_2. \quad (4.1)$$

In Eq. (4.1) $\boldsymbol{\sigma}_i$ and $\boldsymbol{\tau}_i$ are the spin and the isospin vectors, respectively, of each of the colliding particles. The results of the analyses for $(p,p'x)$ and (p,nx) reactions are shown in

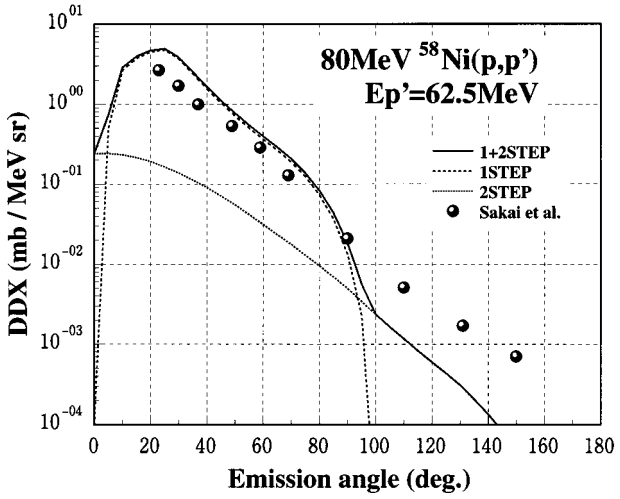

FIG. 5. The same as in Fig. 1 but for $(p,p'x)$ on ^{58}Ni at 80 MeV and $E_{p'}=62.5$ MeV. The data for the excitation energy of 12–16 MeV are from Ref. [29]. The calculation uses the in-medium DA G matrix.

Fig. 7. Each line represents the contribution of each term of Eq. (4.1) to the one-step part of the spin flip. For example, the contribution of V_σ is defined as

$$F(V_\sigma)\equiv\frac{\sigma^{1\text{step}}_{\uparrow\downarrow;V_\sigma}+\sigma^{1\text{step}}_{\downarrow\uparrow;V_\sigma}}{2\times\sigma^{1+2\text{step}}_{\text{unpol full}}}, \tag{4.2}$$

where the numerator is calculated with $V_{12}=V_\sigma(s)\boldsymbol{\sigma}_1\cdot\boldsymbol{\sigma}_2$ only, and the denominator with full V_{12}. In Fig. 7, the total contribution of the two-step process and the total spin flip are also plotted.

For (p,nx), it was found that $V_{\sigma\tau}$, $V_{T\tau}$, and the interference between them make large contributions. The contributions of $V_{\rm LS}$ and $V_{LS\tau}$ to S_{NN} are very small. They are null in N-N scattering in free space, since the quantization axis for the spin, taken to be perpendicular to the scattering plane, is parallel to the orbital angular momentum, and the component of the total angular momentum along that axis is conserved. In N-N collisions in the nucleus that condition is not strictly satisfied since the struck nucleon has an initial momentum in all directions. Actual calculations showed, however, that the contributions of the two-body spin-orbit forces were still less than 1% of the total S_{NN} in the cases under consideration. This is presumably because the momentum of the struck target nucleon is much smaller than that of the incident nucleon. The in-medium effect causes considerable changes in the contributions of $V_{T\tau}$ and the interference between $V_{\sigma\tau}$ and $V_{T\tau}$ to S_{NN}. Since the changes are constructive, they cause a rather drastic change in S_{NN}, and so in D_{NN}.

For $(p,p'x)$, some additional contributions exist. V_T, $V_{\sigma\tau}$, $V_{T\tau}$, and the interference between the last two are particularly important. The in-medium effect causes quite large change in them, but the total S_{NN} does not change so drastically since they happen to be rather destructive.

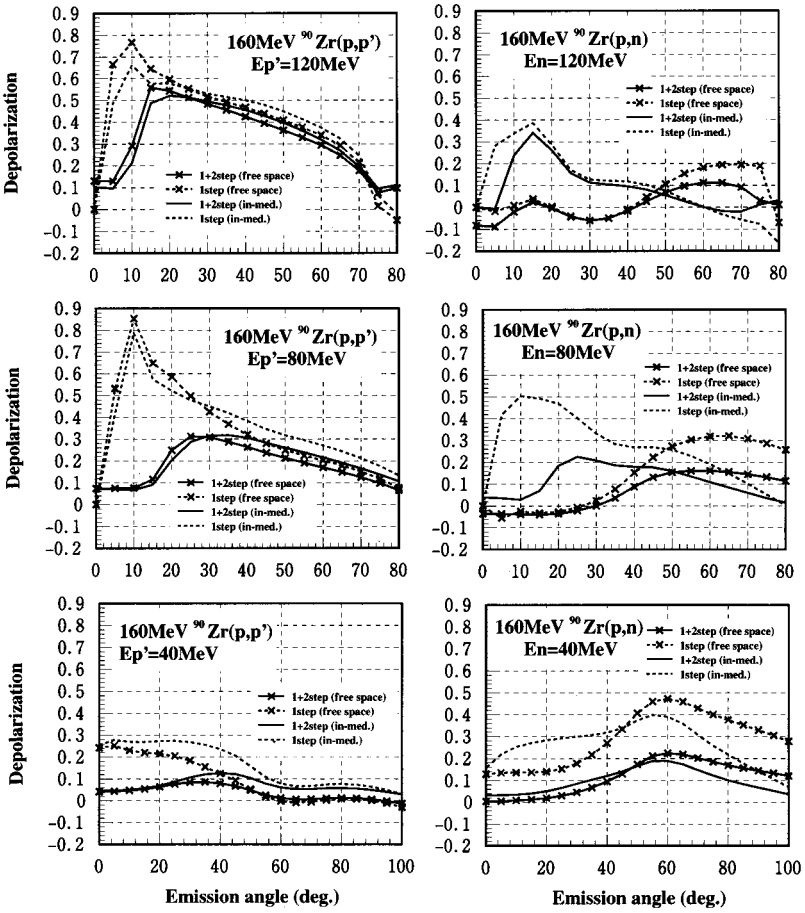

FIG. 6. The same as in Fig. 4 but for $(p,p'x)$ and (p,nx) on ^{90}Zr at 160 MeV for three emission energies of 120, 80, and 40 MeV. The left (right) panel corresponds to $(p,p'x)$ [(p,nx)].

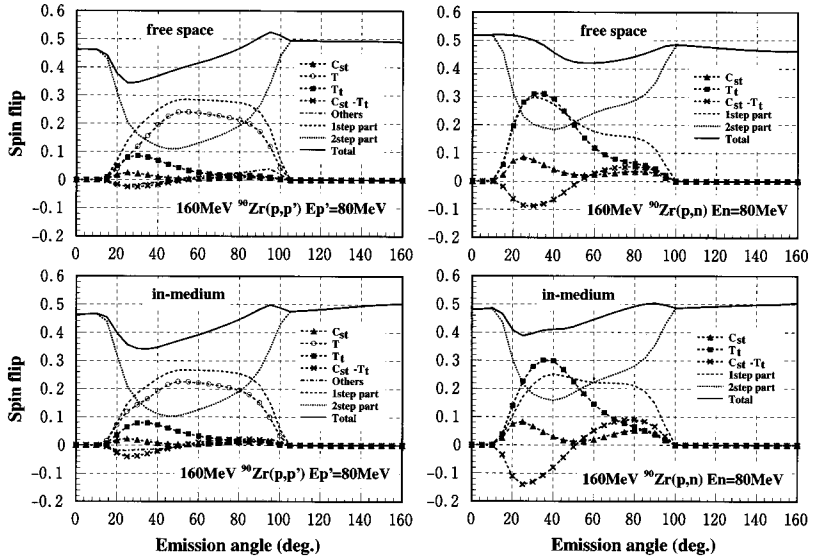

FIG. 7. The contributions of individual components of N-N interaction to the one-step process part of the spin flip in $(p,p'x)$ (left panel) and (p,nx) (right panel) on ^{90}Zr at 160 MeV for the emission energy of 80 MeV. The contribution of two-step process as a whole and the total spin flip are also plotted. The upper and the lower panel correspond to the results obtained with DA ''free space'' and in-medium G matrices, respectively. The contributions of $V_{\sigma\tau}$, V_T, $V_{T\tau}$ of Eq. (4.1) are represented by dashed lines with triangles, open circles, and squares, respectively. Contributions of the interferences between $V_{\sigma\tau}$ and $V_{T\tau}$ are represented by dashed lines with crosses. The lines with no symbol are the total contributions of one-step (dashed lines), two-step (dotted lines), and one-plus-two-step (solid lines) processes. For $(p,p'x)$, the other terms with quite small contributions to S_{NN} are put together and plotted with dash-dotted lines.

V. SUMMARY AND CONCLUSION

The semiclassical distorted wave (SCDW) model is extended to take account of the exchange of colliding particles and to calculate explicitly the off-shell matrix elements with the half-off-shell G matrix parametrized in coordinate representation by Dortmans and Amos (the DA G matrix). Including the exchange term explicitly in the T-matrix element does not change the resultant formula for the double differential inclusive cross section (DDX), which justifies our previous calculations in which the exchange was dealt with only implicitly.

In order to clarify the effects of using exact off-shell matrix elements, the DDXs of $(p,p'x)$ and (p,nx) on ^{90}Zr at 160 MeV are calculated. The agreement with experimental data is almost the same as in our previous work. This justifies our previous calculations with approximate treatment of off-shell matrix elements in terms of on-shell ones. The effect of in-medium modification of the N-N interaction, in-medium effect, on the DDX is examined with the DA G matrix and found to be quite small, in agreement with Ref. [11] in which the effect was investigated with the in-medium N-N cross section given by Kohno *et al.* [30].

The extension in the present paper enables one to calculate spin observables with the SCDW model. We, therefore, calculated the depolarizations D_{NN} and the spin flip S_{NN} for the first time with the SCDW model for ^{58}Ni$(p,p'x)$ at 80 MeV, and for $(p,p'x)$ and (p,nx) on ^{90}Zr at 160 MeV. Numerical tests for one-step process by means of DWBA showed that the spin-orbit coupling in distorting potentials, which is neglected in the present work, little affects D_{NN} and S_{NN} in this case, though significantly affects the polarization and the vector analyzing power. The effect on D_{NN} and S_{NN} of the spin-orbit coupling in the intermediate state distorting potentials in two-step process is also probably unimportant for the reasons discussed in Sec. IV.

The calculated D_{NN} for ^{58}Ni agrees with experimental data in the sign and roughly the magnitude at forward angles, and in qualitative feature of angular dependence. In-medium modification of the N-N interaction improves the agreement at the larger angles.

For (p,nx) on ^{90}Zr, fairly large in-medium effect is observed, in contrast to the case of $(p,p'x)$. Detailed analysis shows that the effect due to the modification of the tensor interaction is particularly important.

In conclusion, the present work put the SCDW model on sounder theoretical foundations than hitherto, and enables calculation of spin observables. Calculations of the depolarization and the spin flip were made for $(p,p'x)$ and (p,nx) and the results were analyzed in detail. The calculated depolarization agrees semiquantitatively with the experimental data on ^{58}Ni$(p,p'x)$ at 80 MeV which are the only available data in middle angular region at present. More extensive and systematic studies of spin observables in $(p,p'x)$ and (p,nx) will be very interesting for the understanding of reaction mechanisms and the refinement of the model. Experimental data, however, are not enough for that purpose, only at a few angles below 20° [31–33] or at 0° [34–36], where the present SCDW model is inadequate. Measurements of D_{NN} in middle angular region is highly desirable.

ACKNOWLEDGMENTS

We wish to express our sincere thanks to Professor K. Amos and Dr. P. J. Dortmans in University of Melbourne for

providing their *G* matrix parametrized in coordinate representation. We also thank Professor Y. Akaishi and Professor Y. R. Shimizu for their kind help on Monte Carlo calculations. We are much indebted to the aid of RCNP, Osaka University, for the computation. The work was partially supported by Grant-in-Aid for Scientific Research of the Ministry of Education, Science, and Culture (Grant Nos. 07640416 and 09558059).

[1] H. Feshbach, A. Kerman, and S. Koonin, Ann. Phys. (N.Y.) **125**, 429 (1980).
[2] N. Nishioka, H. A. Weidenmüller, and S. Yoshida, Ann. Phys. (N.Y.) **183**, 166 (1988).
[3] T. Tamura, T. Udagawa, and H. Lenske, Phys. Rev. C **26**, 379 (1982).
[4] M. L. Goldberger, Phys. Rev. **74**, 1269 (1948).
[5] S. Chiba, M. B. Chadwick, K. Niita, T. Maruyama, T. Maruyama, and A. Iwamoto, Phys. Rev. C **53**, 1824 (1996).
[6] A. Ono, H. Horiuchi, T. Maruyama, and A. Ohnishi, Prog. Theor. Phys. **87**, 1185 (1992).
[7] E. I. Tanaka, A. Ono, H. Horiuchi, T. Maruyama, and A. Engel, Phys. Rev. C **52**, 316 (1995).
[8] Y. L. Luo and M. Kawai, Phys. Lett. B **235**, 211 (1990); Phys. Rev. C **43**, 2367 (1991).
[9] M. Kawai and H. A. Weidenmüller, Phys. Rev. C **45**, 1856 (1992).
[10] Y. Watanabe and M. Kawai, Nucl. Phys. **A560**, 43 (1993).
[11] Y. Watanabe, R. Kuwata, Sun Weili, M. Higashi, H. Shinohara, M. Kohno, K. Ogata, and M. Kawai, Phys. Rev. C **59**, 2136 (1999).
[12] P. J. Dortmans and K. Amos, Phys. Rev. C **49**, 1309 (1994).
[13] H. V. von Geramb, K. Amos, L. Ferge, S. Bräutigam, H. Kohlhoff, and A. Ingemarsson, Phys. Rev. C **44**, 73 (1991).
[14] M. Lacombe, B. Loisseau, J. M. Richard, R. Vinh Mau, J. Côté, P. Pirès, and R. de Tourreli, Phys. Rev. C **21**, 861 (1980).
[15] P. Schwandt, H. O. Meyer, W. W. Jacobs, A. D. Bacher, S. E. Vigdor, and M. D. Kaitchuck, Phys. Rev. C **26**, 55 (1982).
[16] R. L. Walter and P. P. Guss, *in Proceedings of the International Conference on Nuclear Data for Basic and Applied Science*, Santa Fe, New Mexico, 1985, edited by P. G. Young, R. E. Brown, G. F. Auhampaugh, P. W. Lisowski, and L. Stwart (Gordon and Breach, New York, 1986), Vol. 1, p. 1079.
[17] D. G. Madland, *in Proceedings of a Specialists' Meeting on Preequilibrium Reactions, Semmering*, Austria, 1988, edited by B. Strohmaier (OECD, Paris, 1988), p. 103.
[18] F. G. Perey and B. Buck, Nucl. Phys. **32**, 353 (1962).
[19] J. W. Negele, Phys. Rev. C **1**, 1260 (1970).
[20] C. B. Haselgrove, Math. Comput. **15**, 323 (1961).
[21] Y. Akaishi (private communication).
[22] W. A. Richiter, A. A. Cowley, J. J. Lawrie, D. M. Whittal, J. V. Pilcher, and F. D. Smit, Phys. Rev. C **49**, 1001 (1994).
[23] W. Scobel, M. Trabamdt, M. Blann, B. A. Pohl, B. R. Remington, R. C. Byrd, C. C. Foster, R. Bonetti, C. Chiesa, and S. M. Grimes, Phys. Rev. C **41**, 2010 (1990).
[24] W. G. Love and M. A. Franey, Phys. Rev. C **24**, 1073 (1981).
[25] M. A. Franey and W. G. Love, Phys. Rev. C **31**, 488 (1985).
[26] M. B. Chadwick and P. G. Young, Phys. Rev. C **47**, 2255 (1993).
[27] R. Schaeffer and J. Raynal, Program DWBA70 (unpublished); J. Raynal, Nucl. Phys. **A97**, 572 (1967); J. R. Comfort, Extended version DW81 (unpublished).
[28] T. Takahashi, Master thesis, University of Kyoto, 1989.
[29] H. Sakai, K. Hatanaka, N. Matsuoka, T. Saito, A. Shimizu, and M. Ieiri, J. Phys. (France) **55**, 622 (1986).
[30] M. Kohno, M. Higashi, Y. Watanabe, and M. Kawai, Phys. Rev. C **57**, 3495 (1998).
[31] H. Sakai, T. Ichihara, M. Ieiri, K. Imai, N. Matsuoka, T. Motobayashi, T. Noro, T. Saito, A. Sakaguchi, A. Shimizu, and Y. Takauchi, J. Phys. (France) **55**, 624 (1986).
[32] O. Häusser, M. C. Vetterli, R. W. Fergerson, C. Glashausser, R. G. Jeppesen, R. D. Smith, R. Abegg, F. T. Baker, A. Celler, R. L. Helmer, R. Henderson, K. Hicks, M. J. Iqbal, K. P. Jackson, K. W. Jones, J. Lisantti, J. Mildenberger, C. A. Miller, R. S. Sawafta, and S. Yen, Phys. Rev. C **43**, 230 (1991).
[33] J. Lisantti, E. J. Stephenson, A. D. Bacher, P. Li, R. Sawafta, P. Schwandt, S. P. Wells, and S. W. Wissink, Phys. Rev. C **44**, R1233 (1991).
[34] H. Sakai, N. Matsuoka, T. Saito, A. Shimizu, M. Tosaki, M. Ieiri, K. Imai, A. Sakaguchi, and T. Motobayashi, Phys. Rev. C **35**, 1280 (1987).
[35] T. Wakasa, H. Sakai, H. Okamura, H. Otsu, S. Fujita, S. Ishida, N. Sakamoto, T. Uesaka, Y. Satou, M. B. Greenfield, and K. Hatanaka, Phys. Rev. C **55**, 2909 (1997).
[36] T. Wakasa, H. Sakai, H. Okamura, H. Otsu, S. Fujita, S. Ishida, N. Sakamoto, T. Uesaka, Y. Satou, M. B. Greenfield, and K. Hatanaka, Phys. Lett. B **426**, 257 (1998).